*Geophys. J. Int.* (2002) **149,** 413–421

# Anomalous seaward dip of the lithosphere–asthenosphere boundary beneath northeastern USA detected using differential-array measurements of Rayleigh waves

William Menke[1] and Vadim Levin[2]

[1]*Lamont-Doherty Earth Observatory of Columbia University, Palisades,* NY 10964, *USA. E-mail: menke@ldeo.columbia.edu*
[2]*Department of Geology and Geophysics,* Box 208109, *Yale University, New Haven,* CT 06520, *USA. E-mail:vadim@hess.geology.yale.edu*

Accepted 2001 November 21. Received 2001 November 21; in original form 2001 May 8

## SUMMARY

Rayleigh wave phase velocities and azimuth anomalies in the period range of 30–100 s are measured for a set of four triangular arrays of broad-band seismometers in coastal northeastern USA. This is a region in which a strong upper mantle slow shear velocity anomaly (a 'New England Anomaly'), crosses the continental margin. Earthquakes from a wide range of directions are used to detect the variation of parameters with azimuth, $\theta$, of propagation. No lateral heterogeneity in phase velocity is detected at these periods between stations at the centre and the edge of the Anomaly. However, large (10–20 per cent) azimuthal variations occur, and have a $\cos(1\theta)$ dependence, which is indicative of a dipping structure in the upper mantle. Corresponding azimuth variations, with a magnitude of $\pm 5°$, are also detected. This behaviour is consistent with a southeasterly (N150°E) dip of the lithosphere–asthenosphere boundary beneath New England. This dip is associated with the shoaling of the New England Anomaly beneath the Adirondack mountains, west of the array. It is opposite to the dip associated with lithospheric thickening toward the interior of the craton.

**Key words:** anisotropy, continental margin, lithosphere, North America, Rayleigh waves, upper mantle.

## 1 INTRODUCTION

The northeastern edge of North America is a 'textbook-case' passive margin (Grow & Sheridan 1988; Sheridan *et al.* 1995). It was formed during a Mesozoic (0.2 Ga) rifting event that created the Atlantic Ocean, which was associated with voluminous mafic magmatism (see a review in Mahoney & Coffin 1997). It has experienced very little subsequent tectonic activity, the most significant event being the passage of the hotspot that formed the New England sea mounts in the Cretaceous at 0.1 Ga (Sleep 1990) (Fig. 1).

The eastern half of the North American continent consists of sequence of terranes that were progressively accreted to the central Archean craton during the last 3 Gyr. The Grenville province (Moore 1986) formed 1.2 Ga following the closure of a Proterozoic ocean basin. It separates the central craton from the younger (0.3–0.4 Ga) terranes of the Appalachian Orogen that were accreted during the closure of the Iapetus Ocean during the Paleozoic (Taylor 1989).

A general thinning of the continental crust from 45 to 50 km at the centre of the craton to ~35 km at the coast to 15–20 km on the continental shelf is evident from seismic refraction data (Hughes & Luetgert 1992; Hennet *et al.* 1991; Keen & Barrett 1981), also see a compilation by Mooney *et al.* (1998). The subareal thinning mostly reflects the different provenance of the constituent tectonic units, with terranes that accreted more recently generally having a thinner crust. The submarine thinning reflects 40–50 per cent extension during the Mesozoic rifting event that created the present-day Atlantic Ocean (Steckler & Watts 1978).

A corresponding—though less thoroughly studied—thinning of the mantle lithosphere occurs as well. Upper mantle shear velocity models, based on long-period waveform inversion, show a general decrease in lithospheric thickness (as delineated by mantle shear wave velocity) along a traverse from the centre of the craton into the eastern Atlantic (Van der Lee & Nolet 1997). A recent study of mode-converted body waves by Li *et al.* (2002), provides further evidence of this thinning by identifying an eastward decrease in depth of a velocity interface, which is probably associated with the bottom of the lithosphere.

The seismic velocity under cratonic North America is systematically faster than the global average, with the maximum of about 6 per cent occurring in the Great Lakes region (e.g. Grand 1987). Velocities under the eastern North American margin are lower, but the overall pattern is not (as one might expect) margin-parallel. Instead, several smaller-scale (of the order of 400 km) but large-amplitude (±6 per cent) heterogeneities are present, some of which are elongated and nearly perpendicular to the margin (Van der Lee & Nolet 1997) (Fig. 1). Regional *P*-, *S*-wave and surface wave tomographic studies show that this heterogeneity persists at smaller scales as well (Taylor & Toksoz 1979; Levin *et al.*

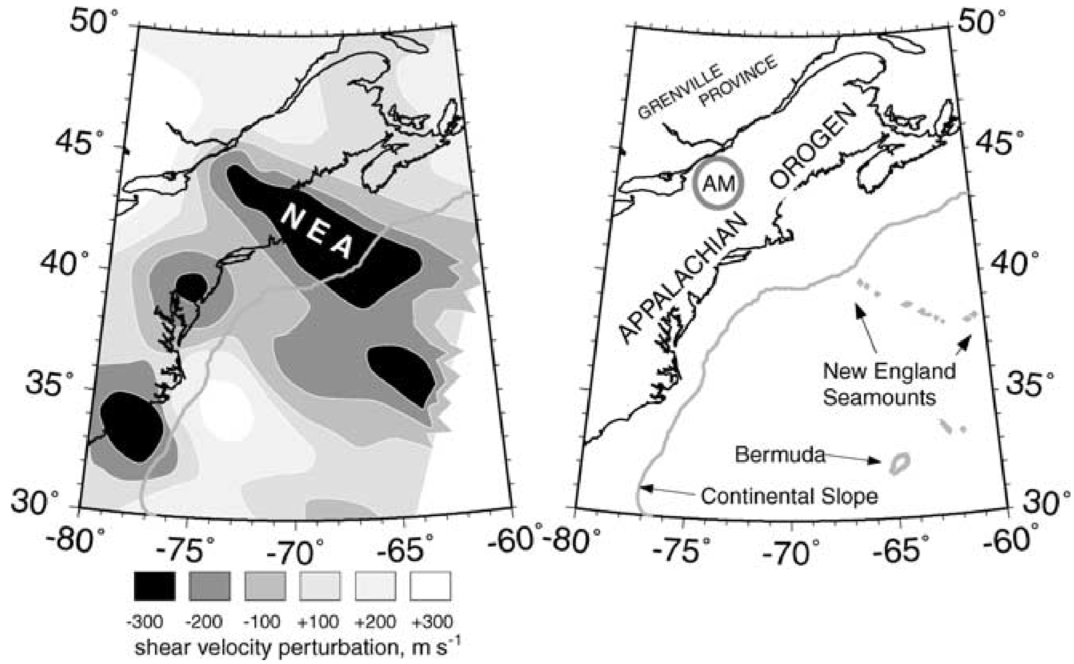


**Figure 1.** Left: shear wave velocity anomalies 100 km beneath the eastern North America passive margin (adapted from Van der Lee & Nolet 1997). Right: tectonic units of the eastern North America passive margin. A depth contour of 2000 m (shaded) outlines the edge of the continent. AM, Adirondack Mountains.

1995; Li, 2002). Interestingly, the high level of velocity heterogeneity has no corresponding analogue in the pattern of shear wave splitting, which is laterally homogeneous (Levin *et al.* 1999, 2000). The velocity heterogeneity must therefore represent 'non-directional' aspects of the mantle structure (composition and/or temperature, not anisotropy).

The most prominent of the margin-perpendicular anomalies is a low-velocity streak that Van der Lee & Nolet (1997) map as extending from beneath the NY Adirondack mountains, across New England, to a point at least 1000 km off shore. Its width is variable, but in the 200–500 km range. It is centred at a depth interval of about 100 km beneath the Adirondacks, deepening to 150 km beneath the Atlantic (see Van der Lee & Nolet 1997, Plates 4 and 5 therein). Its geographical location is roughly coincident with the track of the New England seamounts, leading Van der Lee & Nolet (1997) to postulate that it represents a groove eroded into the lithosphere by the passage of the hotspot. This anomaly, which we will subsequently refer to as the 'New England Anomaly' (NEA), is also evident in Levin *et al.*'s (2000) shear wave tomography (see Fig. 2) and in Aibing Li's (personal communication, 2000) maps of Rayleigh wave phase velocity (although there is only poor agreement on its exact shape).

Imaging techniques, such as the three that have been applied to this region, provide a good overall picture of the lateral heterogeneity. They can, however, suffer from the effects of poor resolution, which can smear features out or project them into incorrect locations. This problem is particularly important with studies carried out on the edges of continents, such as northeastern North America, because of the lack of seismic stations in the oceans. Furthermore, velocity structure and anisotropy can trade-off in complicated ways. Neglecting anisotropy, or assuming, say, a $\cos 2\theta$ pattern with a constant fast direction (as is commonly done) can lead to artefacts in regions where these assumptions are violated.

In this paper we pursue an alternative to tomography, in which we use small seismic arrays to make local measurements of the Rayleigh wave phase velocity and the azimuth of propagation. The advantage of such measurements is that they do not involve tomographic reconstruction, and they do not make prior assumptions concerning anisotropy. The disadvantage, however, is that a separate array is required for each patch of the Earth where a measurement is to be made. Fortunately, sufficient numbers of seismic stations have been operated to allow us to examine a swath of coastal northeastern USA that overlies the NEA anomaly just west of the coastline.

Our primary findings are that: (a) Rayleigh waves in the period range of 30–100 s have similar phase velocities throughout the region that covers the centre and the edge of the NEA; (b) throughout the region phase velocities display a $\cos 1\theta$ dependence on the azimuth of wave propagation, with an amplitude of variation in the 10–20 per cent range; and that (c) the directions of relatively 'fast' and 'slow' Rayleigh wave propagation are 150°SE and 30°NW, respectively. We interpret these findings in terms of the geometry of the lithosphere–asthenosphere boundary beneath the region. We argue that this boundary shoals inland (from the coast towards the Adirondack Mountains), which is anomalous for a passive continental margin setting.

## 2 DATA RETRIEVAL AND PREPARATION

Five seismographic stations (HRV, LBNH, PAL, BINY and SSPA; see Table 1 Fig. 3) in northeastern USA were selected for the analysis, on the basis of their location (east of the edge of the Precambrian craton) and their relatively long interval of operation (at least 5 yr). Broadband vertical-component data from 35 earthquakes, most having magnitudes greater than $M_S = 6$, and with a wide azimuthal distribution, were retrieved from the IRIS Data Management Center; 15 of these earthquakes (Fig. 4 and Table 2) had sufficient station coverage to be used. The instrument response was removed and the resulting velocity records were demeaned, tapered and windowed to isolate the Rayleigh wave. Record sections were inspected visually

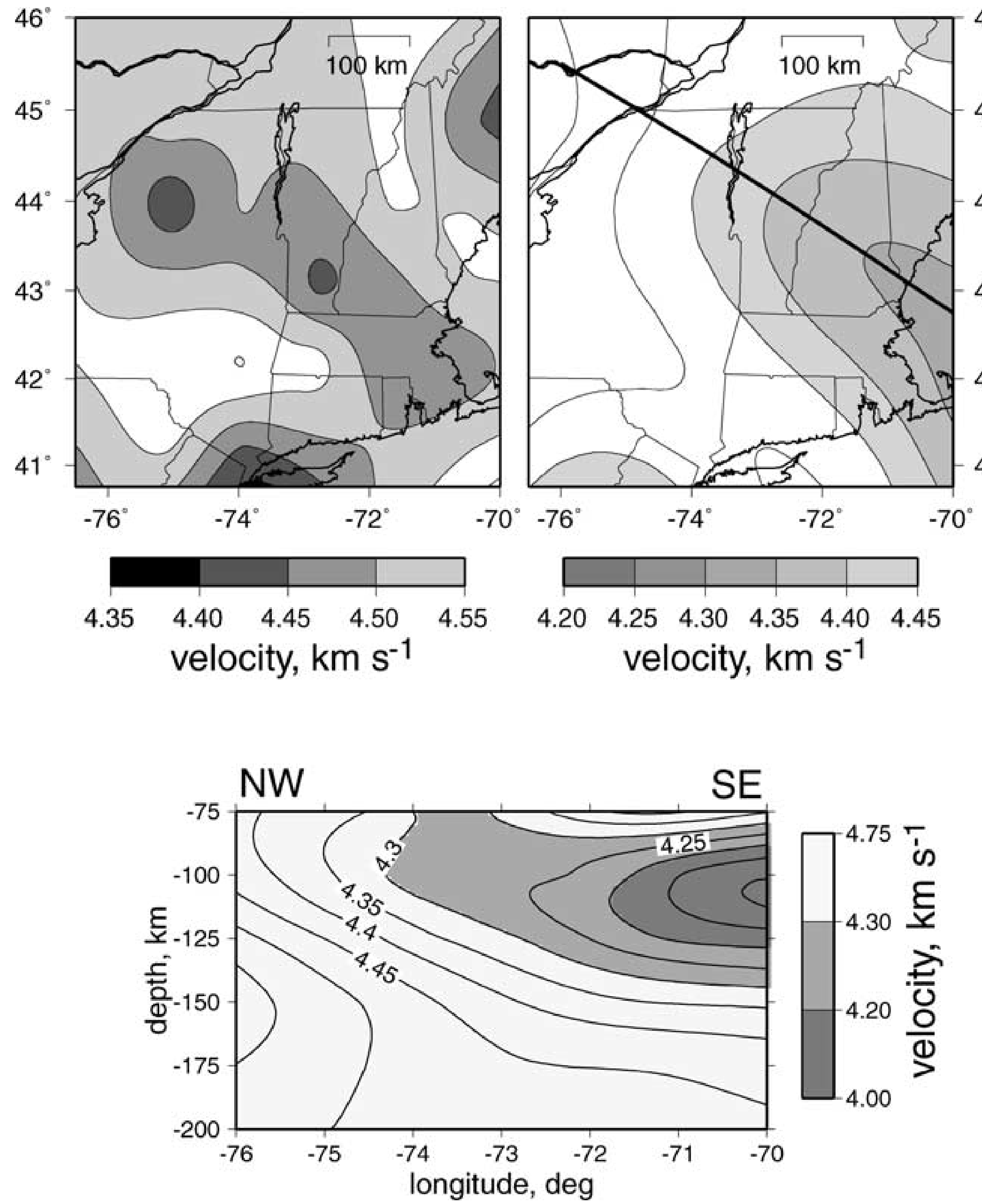


**Figure 2.** Regional variations in shear wave speed at 150 km depth, as imaged by body wave tomography with *S* and *SKS* waves (Levin *et al.* 1999), top left, and Raleigh wave tomography (Van der Lee & Nolet 1997), top right. The solid line on the right-hand panel indicates the trace of the cross-section shown below. There is a general agreement in the trend of the low-velocity features despite large differences in sampling and vastly disparate scales of these studies (body waves, the region shown; Rayleigh waves, continent-wide). Lower panel, vertical cross-section through the NA95 model of Van der Lee & Nolet (1997). Note an 'uplift' of velocity contours towards the interior of the craton.

to identify and fix sign errors and to delete poor quality seismograms (Fig. 5). Rayleigh wave phase velocities were then calculated for four triangular arrays of stations, denoted as T1–T4, as described in the next section. Taken together, these measurements sample a region that extends from central Pennsylvania to southern New Hampshire.

## 3 METHODOLOGY

In this paper we make 'local' estimates of the phase velocity and the direction of propagation of the Rayleigh wave using triangular arrays of seismometers (Priestley & Brune 1978). The measurements are local in the sense that the scalelength over which they are made (typically 100–200 km) is smaller than the wavelength of the Rayleigh waves (200–400 km for 50–100 s waves). Diffraction averages out the effect of small-scale heterogeneity within (and near) the array. Thus the array senses the net movement of a patch of the Rayleigh wave front.

The first step in making the local estimates is to compute the frequency-dependent differential traveltime, $\Delta T_{ij}(\omega)$, of the Rayleigh wave between two nearby stations, $i$ and $j$. We assume that we have a vertical-component velocity seismogram, $s_i(t)$, which has been tapered to remove body wave phases and windowed to start

**Table 1.** Seismic stations used in the study.

| Station name | Latitude (°N) | Longitude (°W) | Operator |
|---|---|---|---|
| BINY | 42.19 | 75.99 | USNSN |
| HRV | 42.50 | 71.56 | GSN |
| LBNH | 44.24 | 71.93 | USNSN |
| PAL | 41.00 | 73.91 | IRIS and LDEO |
| SSPA | 40.640 | 77.89 | GSN |

Abbreviations are as follows: USNSN, US National Seismic Network; GSN, Global Seismic Network; LDEO, Lamont-Doherty Earth Observatory; and IRIS, Incorporated Research Institutions for Seismology.

just prior to the onset of the Rayleigh wave, at a time $\tau_i$ after the origin time of the earthquake. The Fourier transform of the windowed seismogram is $s_i(\omega) = A_i(\omega)e^{i\phi_i(\omega)}$, where $A$ is the amplitude and $\phi$ is the phase. The differential traveltime of the Rayleigh wave is then $\Delta T_{ij} = (\tau_i - \tau_j) - [\phi(\omega)_i - \phi(\omega)_j]\omega^{-1}$. The differential phase, $\Delta\phi_{ij} = [\phi(\omega)_i - \phi(\omega)_j]$ can conveniently be computed by cross-correlating the two seismograms, since the Fourier transform of $s_i(t) * s_j(-t)$ is proportional to $e^{i\Delta\phi_{ij}}$. The use of the cross-correlation also reduces the effort needed to unwrap the phase measurement.

The second step is to make a local estimate of the phase velocity (and possibly also of the azimuth) of the Rayleigh wave using differential traveltimes from several pairs of stations. The simplest strategy is to assume that the azimuth of propagation is approximately given by the azimuth of the great circle connecting the hypocentre to the centre of the array. Then the differential phase is $\Delta T_{ij} = p(\omega)(r_j - r_i)$, where $p(\omega)$ is the phase slowness and $r_i$ is the great-circle distance between the hypocentre and station $i$. Only one measurement of differential traveltime (i.e. two stations) is needed to solve for the phase velocity, $v(\omega) = 1/p$. This estimate will be biased upward, however, if lateral refraction of the Rayleigh wave owing to heterogeneities along its path causes it to arrive off-azimuth.

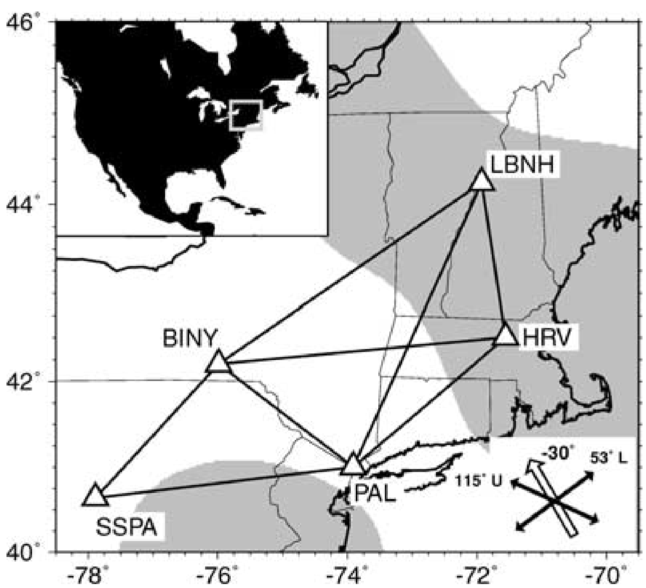


**Figure 3.** Map of broad-band seismic stations (triangles) in northeastern USA used in this study. The stations are grouped into four triangular three-station arrays that are used to make local measurements of Rayleigh wave phase velocity, as follows: (1) PAL–BINY–HRV; (2) PAL–SSPA–BINY; (3) PAL–HRV–LBNH; (4) BINY–HRV–LBNH. Shading shows an area of NA95 model (Van der Lee & Nolet 1997) where shear wave velocity is below 4.35 km s$^{-1}$ at 100 km depth. Orientations of anisotropic symmetry axes in two layers of mantle fabric (Levin *et al.* 1999) are shown by solid arrows (U, upper; L, lower). An open arrow shows the shallowing of the lithosphere–asthenosphere boundary towards 30°NW inferred in this study.

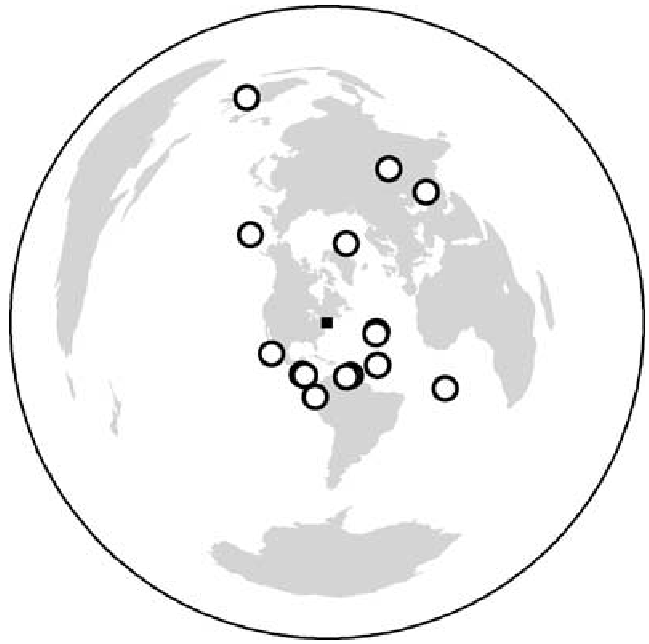

**Figure 4.** Map of earthquakes (circles) used in this study.

The true azimuth can be estimated directly by assuming that the wave front is locally linear, so that the differential traveltime between two stations, $\Delta T_{ij} = \mathbf{p}(\omega)\cdot\Delta\mathbf{x}_{ij}$, where $\mathbf{p}(\omega)$ is the phase slowness and $\Delta\mathbf{x}_{ij}$ is the great-circle distance between the two stations. Two pairs of differential phase measurements (i.e. three stations) are needed to solve for the two unknown components, $p_x$ and $p_y$, of the phase slowness. The phase velocity, $v(\omega)$ is then given by $1/v(\omega) = \sqrt{p_x{}^2 + p_y{}^2}$ and the azimuth of propagation by $\theta(\omega) = \arctan(p_x/p_y)$.

However, if the stations are too close to the epicentre of the earthquake, the curvature of the wave front, which is unaccounted for in the above method, can bias the estimates of phase velocity and

**Table 2.** Earthquakes used in the study.

| Event (dd/mm/yy) | Latitude (deg) | Longitude (deg) | Depth (km) |
|---|---|---|---|
| 23/03/97 | 30.82 | −41.50 | 10.0 |
| 22/04/97 | 11.16 | −61.09 | 47.1 |
| 01/05/97 | 18.99 | −107.34 | 33.0 |
| 10/05/97 | 33.65 | 59.74 | 33.0 |
| 17/06/97 | 51.32 | −179.35 | 33.0 |
| 09/07/97 | 10.50 | −63.54 | 3.0 |
| 21/03/98 | 79.88 | 1.86 | 10.0 |
| 21/05/98 | 0.21 | 119.58 | 33.0 |
| 18/06/98 | −11.57 | −13.89 | 10.0 |
| 04/08/98 | −0.59 | −80.39 | 33.0 |
| 23/08/98 | 11.66 | −88.04 | 54.6 |
| 27/08/98 | 39.66 | 77.33 | 33.0 |
| 01/10/98 | 13.74 | −45.56 | 10.0 |
| 09/10/98 | 11.32 | −86.44 | 68.7 |
| 05/10/00 | 31.64 | −40.83 | 10.0 |

Locations determined by National Earthquake Information Center (NEIC).

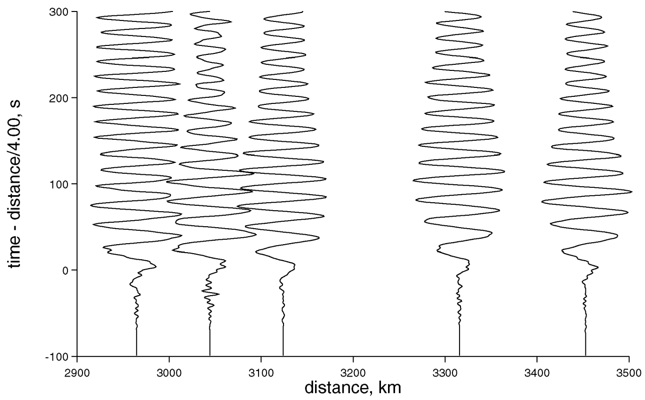


**Figure 5.** Vertical component record section, reduced to 4.0 km s$^{-1}$, of Rayleigh waves from a mid-Atlantic ridge earthquake observed on broad-band stations in northeastern USA. The event occurred on October 5 2000. The seismograms, in order of increasing range, are from HRV, LBNH, PAL, BINY and SSPA.

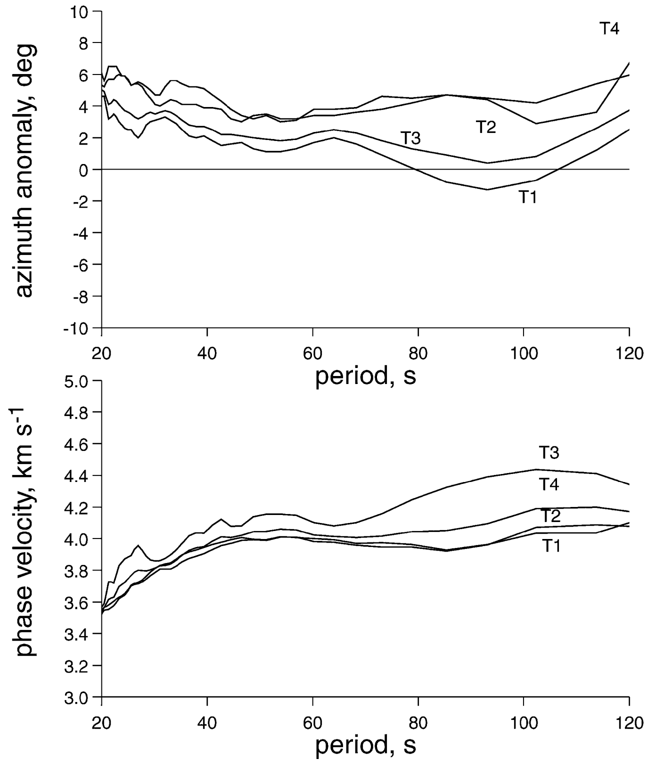


**Figure 6.** Local estimates of azimuth anomaly (with respect to the great circle) and phase velocity for four triangles in northeastern USA to a single earthquake on the mid-Atlantic Ridge. The event occurred on October 5 2000.

azimuth. Furthermore, if the stations are hundreds of kilometres apart, the curvature of the Earth must be accounted for as well. We handle this problem by fixing the curvature of the wave front to its great-circle value, but allow its phase velocity and azimuth to vary. Differential traveltimes from three stations, and distances computed on an elliptical earth, are then used to find the best-fitting values. This approach is only approximate, since the same lateral heterogeneity that causes the Rayleigh wave to arrive off-azimuth will perturb its curvature. However, as the observed azimuth anomalies are typically small ($\leq 5^\circ$), the error in the approximation is negligible.

Since two sets of data (two differential phase measurements) are used to estimate two parameters (two components of horizontal phase velocity), the data can be fitted without error. Thus formal error estimates cannot be provided. However, the stability of the slowness estimates with frequency provides an informal measure of error, since we expect that the phase velocity varies only slowly with frequency. This expectation is met, in general, with our data (see Fig. 6), at least for periods in the 30–100 s range.

## 4 PHASE VELOCITY OBSERVATIONS

The measured phase velocities generally increase with period, following a pattern characteristic of dispersion in a continental setting (Fig. 6). Azimuth anomalies are calculated with respect to the azimuth of the great circle connecting the earthquake epicentre to the centre of the triangle and using the fixed-curvature method. We observe no significant overall bias about an azimuth anomaly of zero (i.e. the mean anomaly for all events and triangles is very nearly zero). However, the magnitude of the typical anomaly grows as the period decreases, from about 3° at 100 s to about 15° at 25 s. This trend probably reflects lateral refraction of the Rayleigh waves owing to variations in crustal thickness, the effects of which are most pronounced at shorter periods.

We concentrate now on the 30–100 s period range, which is sensitive to the shear velocity of the upper several hundred kilometres of the mantle. The variation of phase velocity with azimuth is considerably stronger than its variation between the four triangular arrays (its variance with azimuth is larger than its interarray variance by a factor of 2.1). The azimuthally averaged phase velocity in the 75–100 s period range is 4.06 km s$^{-1}$, with a standard deviation (between triangular arrays) of only 0.06 km s$^{-1}$, or 1.5 per cent. Such a low degree of heterogenity is surprising given the significant upper-mantle heterogeneity that has been detected by other methods (e.g. body wave tomography, Levin *et al.* 2000). On the other hand, the wavelengths involved are very long (120–400 km), so it is possible that the homogeneity arises mainly from the wavefield smoothing effect.

Even more surprisingly, the measured phase velocity is a strong function of azimuth, with propagation to the northwest (i.e. events from the southeast) having a phase velocity that is significantly slower than propagation to the southeast (i.e. events from the northwest) (Fig. 7). The magnitude of this difference is about 20 per cent at a period of 100 s, and declines to about 10 per cent at a 30 s period.

The phase velocity varies strongly with the azimuth, $\theta$, of propagation with a very strong $\cos[1(\theta - \theta_0)]$ component (with $\theta_0 \sim$ N150°E). We interpret this behaviour as being caused by the Rayleigh wave phase velocity being perturbed by a dipping structure in the lithosphere.

The effect of a dipping structure on the propagation of body waves is well understood, because it can be easily modelled with ray theory (see, for example, Lay & Wallace 1995, Box 3.2). A wave propagating in the up-dip direction experiences a steeper velocity gradient than it would in a vertically stratified medium. Its horizontal phase velocity is therefore perturbed to higher values. Conversely, propagation in the down-dip direction causes a perturbation to lower the horizontal phase velocity. The overall pattern of variation with azimuth of propagation varies as $\cos[1(\theta - \theta_0)]$, where $\theta_0$ is the up-dip direction.

Assessing the effect of a dipping structure on a surface wave requires a more complicated analysis (e.g. numerical modelling;

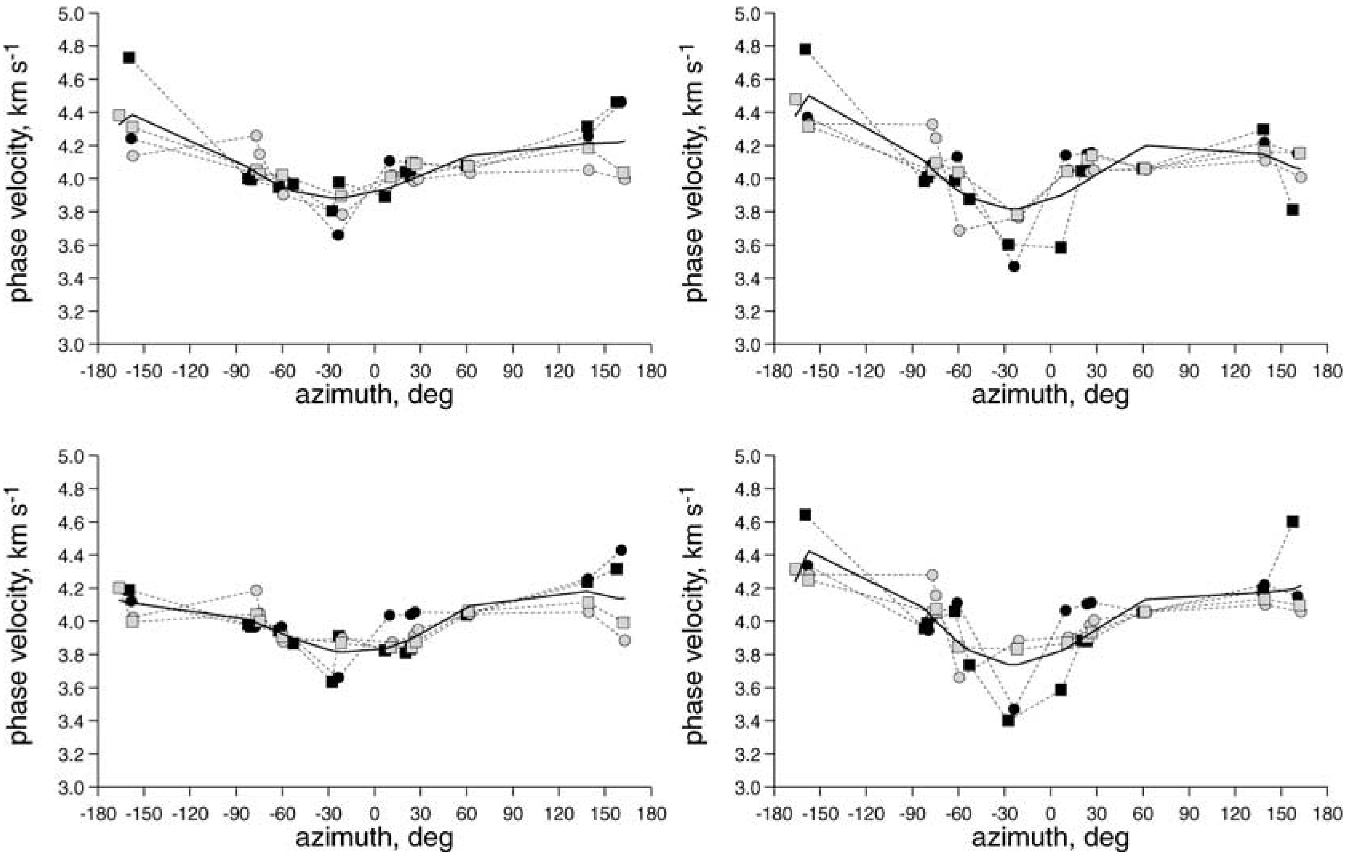


**Figure 7.** Left: variation of the average phase velocity in the 33–50 s interval with azimuth for four trianges of stations in northeastern USA. Top: calculation with azimuth anomaly fixed at zero. Bottom: calculation with fixed wave front curvature and variable azimuth. Each symbol represents a single earthquake observed on a single triangle of stations (black circles, T1; black squares, T2; grey circles, T3; grey squares, T4; see Fig. 3 for triangle definitions). The bold curve is a smooth polynomial fit to all the data. *Right*, Same for period range 75–100 s.

see Smith 1974). Nevertheless, the fundamental physical principle of the phase velocity being perturbed to higher values in the up-dip direction is the same in both the body and surface wave cases. Bullen & Bolt (1985) (Section 12.3.3) describe the result of a numerical calculation for fundamental-mode Love waves interacting with a dipping boundary. As the waves propagate up-dip, the effect of the phase velocity perturbation is to cause forward scattering into higher modes (which, for a given frequency, have a faster phase velocity than the fundamental mode). An array of seismometers placed above a dipping boundary cannot discriminate between the several modes. Instead it detects an overall phase velocity that is somewhat faster than in the vertically stratified case.

Although only the Love wave case appears to have received attention in the literature, we expect a similar result to hold for the Rayleigh waves that we study here. We note that while the observed $\cos(1\theta)$ azimuthal behaviour of the phase velocity is consistent with a dipping structure, it is not consistent with that expected from the anisotropic variation of wave speed, which has $\cos(2\theta)$ and $\cos(4\theta)$ components.

The azimuths of the slow and fast directions are about $-30^\circ \pm 10^\circ$ and $150^\circ \pm 10^\circ$, respectively. Average dispersion curves for these two directions are shown in Fig. 8. The slow-direction dispersion curve is particularly interesting, because it has reverse dispersion for periods greater than about 60 s. Unfortunately, while the precise velocity structure implied by the dispersion curves in Fig. 6 is of great interest, we know of no inversion procedure that can properly account for strong lateral gradients in structure.

The azimuth anomaly measurements (Fig. 9) are consistent with the inferred dipping structure, especially in the 75–100 s period range which is least sensitive to crustal heterogeneity. The lateral gradient (i.e. a change from slower to faster phase velocities) causes an azimuth anomaly because the Rayleigh wave propagation direction tends to curve away from the direction of maximum lateral velocity gradient (Fig. 10). Propagation exactly along (or exactly towards) the lateral gradient yields no azimuth anomaly. Propagation

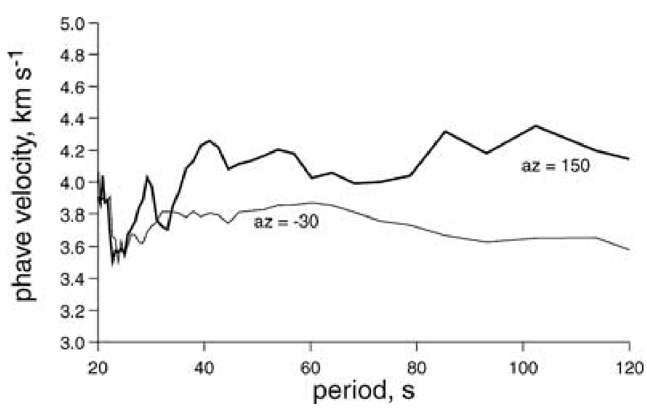


**Figure 8.** Phase velocity as a function of frequency for the antiparallel azimuths of $-30^\circ \pm 15^\circ$ and $150^\circ \pm 15^\circ$. Data for all events in these azimuth ranges recorded by all four triangles have been stacked. Note the large difference in phase velocity for waves travelling in opposite directions.

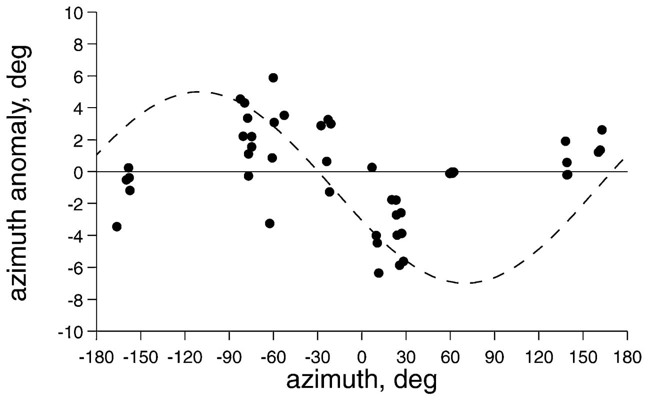


**Figure 9.** Variation of the azimuth anomaly (with respect to the great circle) in the 75–10 s interval with azimuth for trianges of stations in northeastern USA. Calculation with fixed wave front curvature. Each symbol represents a single earthquake observed on a single triangle of stations. Dotted curve is a best-fitting cos($1\theta$) curve.

at other azimuths leads to either a positive or a negative anomaly, depending upon the side of the gradient direction the path is on. This antisymmetric pattern is clearly detected in the data around the $-30°$ direction. Insufficient data are available to confirm the pattern for the 150° case.

We would expect that the azimuth anomalies would also be detectable through measurement of the azimuth of Rayleigh wave particle motion (e.g. by using the multitaper spectral estimation technique of Lerner-Lam & Park 1989). However, successful application of that technique requires both very accurate calibration of the horizontal seismometer responses and seismograms especially selected to avoid the interfering effect of Love waves (which have large horizontal motions in the relevant period range). Thus we have not pursued such measurements here.

## 5 INTERPRETATION AND CONCLUSIONS

Our observations indicate that the Rayleigh wave phase velocity in the northeastern USA exhibits a lateral gradient that points towards

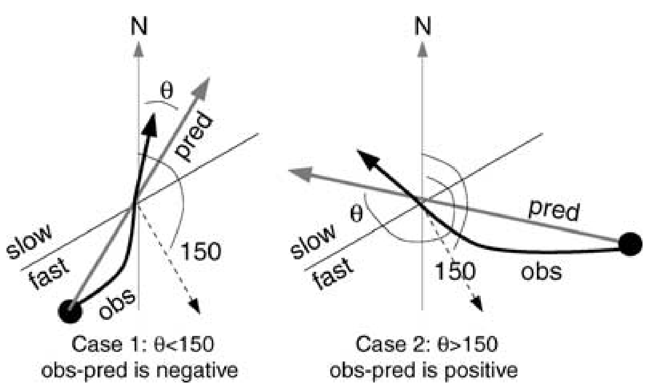


**Figure 10.** A lateral gradient (i.e. a change from slower to faster phase velocities) in velocity structure (dashed vector) is associated with a pattern of azimuth anomalies that are antisymmetric about the azimuth of the vector (here 150°). The direction of propagation of the waves curves away from the faster velocities (bold black curve), leading to an observed azimuth that is different than that predicted on the basis of the great-circle path (bold grey line). The sign of the azimuth anomaly is different for sources on the two sides of gradient vector direction.

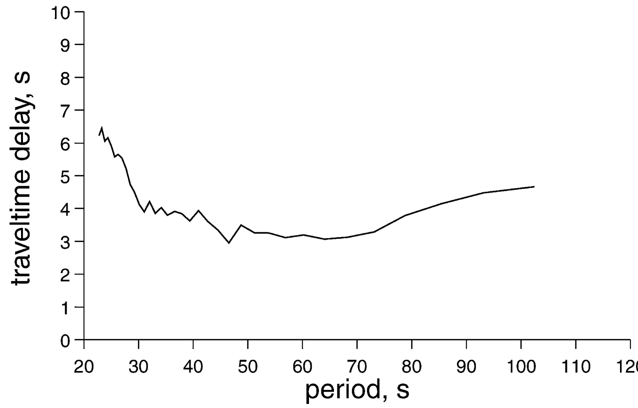


**Figure 11.** Differential traveltime between HRV and PAL for a Rayleigh wave from the 2000 October 5 mid-Atlantic Ridge earthquake, after a correction that adjusts the two stations to the same source–receiver range. The delay of arrival at HRV by about 4 s reflects propagation along a path that is about 3 per cent slower than the path to PAL, an amount consistent with path to HRV being through the centre of the New England Anomaly and the path to PAL being along its southern edge.

the southeast (towards the coast). This behaviour is precisely the opposite of what one would expect for a 'normal' continental margin, where the lateral velocity gradient would be expected to point into the cold interior of the craton (i.e. a seismically faster lithosphere within the craton). It is, however, exactly the signal expected from the NEA, and especially from the slow shear velocities beneath the Adirondacks.

The along-coast extent of the region in which we detect the cos($1\theta$) phase velocity variation is wider, by a factor of at least 2, than the NEA. To some degree, this difference may reflect the lateral averaging of the long-period Rayleigh waves and the choice of reference models by which the velocity anomaly is defined. However, it may also indicate that NEA is wider than has previously been recognized.

The 2000 October 5 mid-Atlantic Ridge earthquake is in a location favourable for detection of the seaward part of the NEA, since the path to HRV passes through the centre of the oceanic portion of the NEA, while the path to PAL passes along its southern edge. After correcting for the slightly different ranges of the two stations (by applying the dispersion curve measured at triangle 1 to adjust PAL traveltimes), waves at HRV are found to be delayed by 4–5 s with respect to PAL in the 30–100 s period band (Fig. 11). This delay implies that velocity along the hypocentre–HRV path is about 3 per cent slower than along the hypocentre–PAL path. The delay is consistent with the seaward path of the NEA, as mapped by Van der Lee & Nolet (1997). This measurement demonstrates that the seaward part of the NEA is not an artefact of the tomographic reconstruction. It can be detected using only coastal stations, and by comparing two very similar propagation paths.

These results provide strong evidence that the low shear velocities beneath the Adirondacks extend continuously across New England to connect to a somewhat deeper low-velocity anomaly offshore. The alternate interpretation, that these are two distinct anomalies that have been smeared together by the tomography, is discounted.

The NEA cuts across the continental margin, indicating that it post-dates the 200 Ma opening of the Atlantic Ocean. Shear wave splitting studies that use core-converted phases such as *SKS* indicate that northeastern USA has two distinct, laterally homogenous layers of mantle fabric. The shallower layer, about 60 km thick, has a fast axis of N115°E, and the deeper layer, about 90 km thick, has a fast axis of N53°E (Fig. 3). The *SKS* data do not constrain the actual depth of these layers, except to place them above the transition zone (i.e. above 400 km). Orientation of the fast axis in the lower layer is in good agreement with the absolute plate motion of the North American plate, and is likely to represent the present-day strain in the asthenosphere. Consequently, Levin *et al.* (1999) argued that the top layer of fabric has to be within the consolidated mantle lithosphere of the North American continent.

The NEA does not disrupt (or otherwise alter) either of these layers. The splitting measurements are based on relatively short period (<5 s) measurements and sample a relatively small patch of mantle (<50 km) beneath each seismic station. Thus the smoothing of lateral variations by wavefield diffraction cannot explain the homogeneity of the splitting measurements. They imply a real homogeneity of anisotropic fabric that extends from the centre of the NEA in Massachusetts to its edge in southern New York.

One possibility is that the anisotropic layers are at different depths in the mantle from the low shear velocities associated with the NEA. The data do not preclude the upper layer being wholly above the NEA, and the lower layer being wholly below it (or, alternatively, both layers being below it). Indeed, the absence of any $\cos 2\theta$ or $\cos 4\theta$ variability in Rayleigh wave phase velocity, at least in the 30–100 s period range, strongly suggests that the 100–200 km depth interval is not strongly anisotropic.

Another possibility is that the anisotropic layers represent a strain event that is superimposed upon the NEA and its surroundings, and thus post-dates it. This scenario would argue against the upper layer having anything to do with the Appalachian Orogeny. Except for the hotspot that created the New England Seamounts, and present-day plate motions, no major post-rifting strain events have been reported for this region.

We discount the possibility that the NEA is the cause of either layer of anisotropy. First, the layers extend over a wider geographical region than the NEA. Second, the axis of the NEA, measured from Van der Lee & Nolet's (1997) map, is about N135°E, which is significantly different from anisotropic symmetry axes within either of the anisotropic layers. Mantle flow along the axis of the NEA would not give rise to either fabric. Indeed, we feel that the general lack of any anisotropic signal associated with the NEA argues against it being a result of flow of the asthenosphere into a groove in the lithosphere left by the New England hotspot. Such a flow would need to have occurred over the past 0.1 Ma in order to counteract the conductive cooling of this shallow asthenosphere. Certainly there is no geological evidence for post-Cretaceous thermal subsidence of this region.

In summary, this work contributes further evidence for the existence of the NEA, a major shear velocity anomaly in the upper mantle, and supports the hypothesis that it cuts across the continental margin of northeastern North America. However, it only adds to the mystery of the origin of the anomaly. The seaward dip of the base of the lithosphere from its shallowest point beneath the Adirondack mountains is clearly detected by the azimuthal variation of Rayleigh wave phase velocities and azimuth anomalies. However, no comparable anisotropic signal is present, such as might be associated with irregularities in asthenospheric flow in and near the NEA.

Finally, these results have implications on the conduct of regional Rayleigh wave inversions in which the station spacing is as fine as the values of 100–200 used in this paper. At these scales, we have shown that dipping structures can have a very strong effect on Rayleigh wave phase delays, which are the dispersive equivalent of traveltimes. (At larger scales, the effect of the crossing of a wave both up-dipping and down-dipping structures probably averages out.) Furthermore, the pronounced $\cos 1\theta$ behaviour is at variance with standard tomographic reconstruction techniques which assume that parallel paths in opposite directions are equivalent. Modifications to the inversion algorithm to explicitly account for these effects will probably improve the reliability of the images significantly.

## ACKNOWLEDGMENTS

This research was supported by the NSF grant EAR-9805206 (VL). Aibing Li kindly provided preprints of her work prior to publication, and Susan van der Lee supplied a subset of the NA95 model. Helpful reviews by Susan Van der Lee and an anonymous reviewer are appreciated. We used GMT software (Wessel & Smith 1991) to prepare some figures.

## REFERENCES

Bullen, K.E. & Bolt, B., 1985. *An Introduction to the Theory of Seismology,* 4th edn, Cambridge University Press, Cambridge.

Grand, S.P., 1987. Tomographic inversion for shear velocity beneath the North American Plate, *J. geophys. Res.,* **92,** 14 065–14 090.

Grow, J. & Sheridan, R., 1988. US Atlantic continental margin: a typical Atlantic-type or passive continental margin, in *The Geology of North America I-2,* pp. 1–12, ed. Sheridan, R., Geological Society of America.

Grow, J. Bowin, C. & Hutchinson, D., 1979. The gravity field of the US Atlantic continental margin, *Tectonophysics,* **59,** 27–52.

Hennet, C., Luetgert, J. & Phinney, R., 1991. The crustal structure in central Maine from coherency processed refraction data, *J. geophys. Res.,* **96,** 12 023–12 037.

Hughes, S. & Luetgert, J., 1992. Crustal structure of the southeastern Grenville province, northern New York and Eastern Ontario, *J. geophys. Res.,* **97,** 17 455–17 479.

Keen, C. & Barrett, D., 1981. Thinned and subsided continental crust on the rifted margin of eastern Canada, crustal structure, thermal evolution and subsidence history, *Geophys. J. R. astr. Soc.,* **65,** 443–465.

Lay, T. & Wallace, T., 1995. *Modern Global Seismology,* Academic Press, San Diego, CA.

Lerner-Lam, A. & Park, J., 1989. Frequency-dependent refraction and multipathing of 10–100 second surface waves in the western Pacific, *Geophys. Res. Lett.,* **16,** 527–530.

Levin, V., Lerner-Lam, A. & Menke, W., 1995. Anomalous mantle structure at the Proterozoic–Paleozoic boundary, *Geophys. Res. Lett.,* **22,** 121–124.

Levin, V., Menke, W. & Park, J., 1999. Shear wave splitting in the Appalachians and the Urals: a case for multilayered anisotropy, *J. geophys. Res.,* **104,** 17 975–17 987.

Levin, V., Menke, W. & Park, J., 2000. No regional anisotropic domains in the northerneastern US Appalachians, *J. geophys. Res.,* **105,** 19 029.

Li, A., 2000. Crust and mantle discontinuities, shear wave velocity structure, and azimuthal anisotropy beneath North America, *PhD thesis,* Brown University, Providence, Rhode Island.

Li, A., Fischer, K.M., Van Der Lee, S. & Wysession, M.E., 2002. Crust and upper mantle discontinuity structure beneath eastern North America, *J. geophys. Res.,* in press.

Mahoney, J. & Coffin, M. (eds), 1997. Large igneous provinces: continental, oceanic, and planetary flood volcanism, *Geophysical Monograph 100,* American Geophysical Union.

Mooney, W.D., Laske, G. & Masters, T.G., 1998. Crust 5.1: a global crustal model at 5 × 5 degrees, *J. geophys. Res.,* **103,** 727–747.

Moore, J.M., 1986. Introduction: the Grenville Province then and now, *Can. Geol. Assoc. Spec. Pap.,* **31,** 1–11.

Priestley, K. & Brune, J.N., 1978. Surface waves and the structure of the Great Basin of Nevada and western Utah, *J. geophys. Res.,* A, *Space Phys.,* **83,** 2265–2272.

Sheridan, R., Musse, D., Holbrook, S. & Glover, L., 1995. Mid-Atlantic Coastal Plain and continental margin: basement and mantle structure and continent–ocean transition, in *Centennial Continent/Ocean Transect,* **19,** 69–78.

Sleep, N., 1990. Monteregian hotspot track: a long-lived mantle plume, *J. geophys. Res.,* **95,** 21 983–21 990.

Smith, W.D., 1974. A non-reflecting plane boundary for wave propagation problems, *J. Comput. Phys.,* **15,** 487, 492–503.

Steckler, M. & Watts, A., 1978. Subsidence of the Atlantic-type continental margin off New York, *Earth planet. Sci. Lett.,* **41,** 1–13.

Taylor, S.R., 1989. Geophysical framework of the Appalachians and adjacent Grenville Province, in *Geophysical Framework of the Continental United States,* eds Pakiser, L.C. & Mooney, W.D., *Mem. Geol. Soc. Am.,* **79,** 317–348.

Taylor, S.R. & Toksoz, M.N., 1979. Three-dimensional crust and upper mantle structure of the northeastern United States, *J. geophys. Res.,* **84,** 7627–7644.

Van der Lee, S. & Nolet, G., 1997. Upper mantle *S* velocity structure of North America, *J. geophys. Res.,* **102,** 22 815–22 838.

Wessel, P. & Smith, W.H.F., 1991. Free software helps map and display data, *EOS, Trans. Am. geophys. Un.,* **72,** 441, 445–446.